

The Interpolation of Hydraulic Head Contours

Kelly M. Knapp
Department of Mathematics & Computer Science
Ursinus College
Advisor/Sponsor: Dr. Linda C. Thiel

1	<i>Introduction</i>	2
2	<i>Background</i>	2
2.1	Physical Conditions	2
2.2	Elementary Quantitative Concerns	2
3	<i>Interpolation Techniques for Large Amounts of Scattered Data</i>	4
3.1	The Problem	4
3.2	Techniques Based on Nearest Neighbors	5
	A Simple Linear Method	5
	Ranked Inverse Weighted Distance Method	6
	Inverse Weighted Distance Method	7
	Weighted Average of Nearby Points	8
	Advantages & Disadvantages	9
3.3	Relaxation — Solving Finite-Difference Equations	9
3.4	Test of Starting Conditions	11
3.5	Relaxation Method Applied to Known Test Functions	14
3.6	Relaxation Method Applied to Real Data	17
4	<i>Summary of Results</i>	20
5	<i>Future Study</i>	21
	<i>References</i>	21

1 Introduction

Mathematical models are widely used in many areas of environmental science. In particular, models have been developed to conceptualize groundwater flow. The data necessary for these models is typically drawn from a limited number of wells distributed throughout a geographic region of interest. One of the measurements commonly needed is the hydraulic head, which refers to the height of the water level at any point above a specified plane, typically sea level. From this scattered data, a hydraulic head contour map is developed that depicts where the hydraulic head values are the same. This diagram can be used to determine the direction and velocity of groundwater flow at any point in the region. With this knowledge, it is then possible to ascertain where contaminants in the groundwater may be coming from and in what direction they are flowing. Because most analysis begins with this contour map, it is important to convert data that may come from very limited sources into an accurate contour map.

This paper focuses on methods of interpolation for calculating the hydraulic head contour lines from wells located throughout a region. Several methods of interpolation are discussed, but the emphasis is on relaxation—a finite-difference method. Various methods of initializing the data for use with relaxation are developed in order to represent varying boundary and interior data conditions. The goal is to determine a method that will enhance convergence. After testing the initialization methods on the scattered data set, test functions are used to simulate the situation. Hydraulic head contour maps are created from the data generated for three different scenarios. The results obtained by varying the initial conditions for computing a hydraulic head contour map are presented in both visual and analytical format. The benefits and drawbacks of each method are presented.

2 Background

2.1 Physical Conditions

Before devising a mathematical model, it is necessary to understand the physical conditions leading to the development of the model. If you begin digging a hole at any point on earth and eventually you will strike water. This water, which originates as surface water or precipitation, collects to a certain height between the spaces in soil and rock. The height to which it rises is known as the water table and any water below the water table is referred to as groundwater.

Water enters the water table at the recharge zone. When precipitation falls, it seeps into the ground and eventually enters the water table. Similar conditions exist at a pond; a portion of the pond water can be expected to flow through the ground until it too enters the water table. Surface water bodies, such as ponds, lakes, or streams, do not merely serve as recharge zones; they may also act as discharge zones. Water may seep out of the water table back into a creek via the creek bed (Hadlock, 1998a, chap. 2.2).

Groundwater does not sit stagnantly beneath the soil; it is constantly moving between the water table and surface water bodies. Portions of the underground that allow water to move fairly easily are known as aquifers. Aquifers may be composed of soils, which are particulate, or bedrock, which is solid rock. Soils such as sand and gravel form the most common aquifers, while sandstone and limestone make the most likely bedrock aquifers (Hadlock, 1998a, chap. 2.2). Aquifers may be described as either isotropic or anisotropic. Isotropic aquifers are those in which the geologic medium does not force groundwater to flow in any direction other than where it would ordinarily tend to flow. Anisotropic aquifers, however, favor flow in one direction over another (Hadlock, 1998a, chap. 5.6). Although aquifer formations typically follow the general topography of a region, flow patterns may be substantially different due to complex aquifer formations (Hadlock, 1998a, chap. 2.2). For all purposes in this paper, it will be assumed that aquifers follow the topography of the land and that they are isotropic.

2.2 Elementary Quantitative Concerns

With such a great deal of movement occurring between the water table and surface water bodies, it is highly probable that if a contaminant enters the water supply, numerous water sources could be affected. In fact, there could be disastrous consequences for drinking water supplies. Thus, it is necessary to understand several key quantitative concepts.

Suppose a chemical spill occurred near your house. Naturally, you would want to know how much of the chemical had spilled and how long it had been leaking. Because anything that spills into the ground will eventually enter the water table, you would want to know in what direction and how quickly the groundwater beneath the spill was flowing. Based upon the answers you collect to these questions, you would then want to gauge the accuracy of

the scenario you have predicted. The questions above can be answered after resolving two more basic questions: how much groundwater is flowing through a section of the aquifer and how fast is that water moving? (Hadlock, 1998a, chap. 2.3)

In order to determine how much groundwater flows through a particular section of an aquifer, one must refer to an equation known as Darcy's law (Hadlock, 1998a, chap. 2.4). This equation captures the proportionality inherent in the relationship between the total volumetric flow rate, Q , and several properties of groundwater. The one-dimensional version of Darcy's law may be summarized as

$$Q = -K \frac{\Delta h}{\Delta x} A \quad (2.1)$$

where

h = hydraulic head or height of the water at any point

Δh = change in hydraulic head between two sampling wells

Δx = distance between the two wells

$\frac{\Delta h}{\Delta x} = i$ = hydraulic gradient

A = cross-sectional area of the aquifer

K = hydraulic conductivity constant.

It should be noted that K is dependent upon the geologic composition of the aquifer. It has low values for bedrock and high values for soils. Although hydraulic head is actually the measure of several physical components, note that for the purposes of this paper head value will refer simply to the height of the water (Hadlock, 1998a, chap. 2.4).

Assuming that the aquifer is isotropic and that the groundwater is flowing through a unit cross section of the aquifer (i.e. $A=1$), Darcy's law appears as

$$q = K \frac{\Delta h}{\Delta x} \quad (2.2)$$

or in its differential form

$$q = -K \frac{dh}{dx} \quad (2.3)$$

where the lowercase q denotes that the flow is through a unit cross-sectional aquifer. For the multidimensional case, Darcy's law is rewritten as

$$q = -K \nabla h \quad (2.4)$$

where

$$\nabla h = \left\langle h_x, h_y \right\rangle.$$

Note that the hydraulic gradient $\frac{dh}{dx}$ has been replaced by ∇h , the gradient vector of the function defined by $h(x,y)$. Recall from multivariate calculus that the gradient is a vector composed of the two partial derivatives of a function $h(x,y)$ (Stewart, 1995, p. 804). The physical relationship described by the above equations is that "the flow rate at any point is proportional to the rate of change of head along the flow path at that point (Hadlock, 1998a, chap. 5.6)."

To determine the velocity of the groundwater flowing through an aquifer, one should consult the interstitial velocity equation. This equation determines the velocity of the water through a unit cross-sectional area of an aquifer. It appears as

$$v = \frac{-K \frac{dh}{dx}}{\eta} \quad (2.5)$$

for the one-dimensional case or as

$$v = \frac{-K \nabla h}{\eta} \quad (2.6)$$

for the multi-dimensional case. Equations 2.5 and 2.6 can be written in the more concise form

$$v = \frac{Ki}{\eta} \quad (2.7)$$

Recall that K is the hydraulic conductivity constant and i is the hydraulic gradient. The parameter η is the porosity, or fraction of the geologic medium that is open space. Naturally, this value depends on upon the composition of the aquifer in question (Hadlock, 1998a, chap. 2.5).

Determining the amount of time necessary for groundwater to travel from one point to another requires the use of a basic equation from physics. Simply

$$\text{time} = \frac{\text{distance}}{\text{velocity}}$$

or

$$t = \frac{d}{v}. \quad (2.8)$$

In order to calculate any of the above equations, it is first necessary to drill sampling wells to collect data. Because drilling these wells is quite costly and not always environmentally sound, it is unreasonable to drill large numbers of wells haphazardly throughout a region. By consulting geological and hydrological references, a round of wells can be drilled that will provide a maximum amount of information with a minimal amount of drilling. An initial model of the groundwater flow can be generated from this data, with more wells being drilled later if refinements are necessary.

The data collected from sampling wells is typically organized into a hydraulic head contour map. The lines depicted on the contour diagram show points where the hydraulic head values are the same. Since data from wells within a region is limited, it should be apparent that generating a contour map from this data is largely left to interpolation or extrapolation.

After a contour map has been created, it is possible to add groundwater flow lines. As a rule, the groundwater at any point usually flows in a direction perpendicular to the hydraulic head contour lines. This means that the water is following the path of steepest descent through the water table. An accurate contour map will enable an accurate representation of groundwater flow. If the contours are inaccurate, the results garnered from the contour map could be grossly incorrect. Thus, it is crucial that the methods used to interpolate the well data are precise enough to accurately model the region.

3 Interpolation Techniques for Large Amounts of Scattered Data

3.1 The Problem

Although it is easy to construct a contour line from three data points, real life situations are more complicated. The geographic region that requires analysis may cover an area of several square miles or even several hundred square miles. If this is the case, three sampling wells will not give an adequate amount of information to construct a reasonable contour map. The region would instead require a larger number of wells. Despite having a larger data set to work with, it is still not enough information alone to construct a contour map. The given data serves as a starting point for using interpolation methods to calculate any other unknown hydraulic head in the region. If enough data is generated, it will be possible to construct accurate contour lines.

In *Mathematical Modeling for the Environment*, Charles Hadlock challenges the reader to develop techniques to determine the unknown head values at points A, B, and C in Figure 3.1-1.

The general situation to be investigated...[is represented by Figure 3.1-1], which shows a 5000 ft by 5000 ft geographic area within which a number of wells have been drilled and then measured to determine the hydraulic head at each of their locations. In particular, 24 wells are available and the measured head values range from a low value of 203.2 feet to a high value of 268.2 feet. This kind of well distribution would not be uncommon in this roughly mile square region; and, in fact, the wells might at least in part represent wells drilled in the past for a diversity of purposes, such as drinking water, irrigation water, contaminated plume sampling, or water supply investigation. They are all shown in the figure to be located at grid points on a 500-foot grid pattern, but this is only to simplify their use in later computations.

(1998a, p. 180)

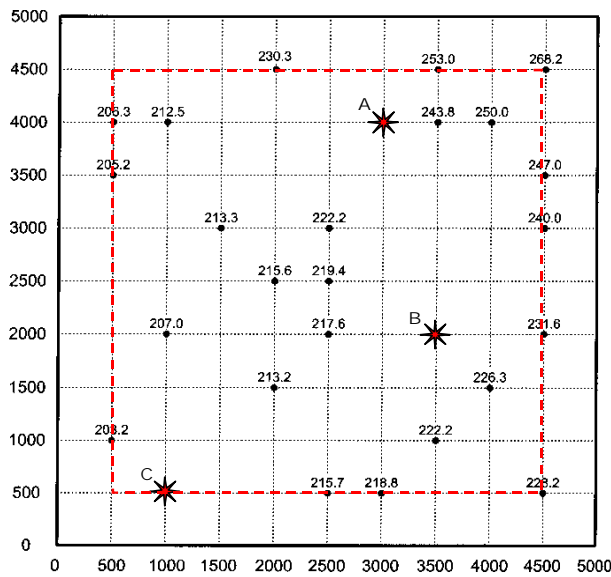


Figure 3.1-1—A typical situation involving multiple wells (Hadlock, 1998a, fig. 5-13).

This case serves as the basis for my work. I devised three of my own methods and also examined one of techniques that Hadlock suggested. These four methods were rejected in favor of the method of relaxation, to be discussed later. The methods are applied to the data given in Figure 3.1-1 and to two other sets of data.

3.2 Techniques Based on Nearest Neighbors

As stated in Section 2.1, the water table generally follows the topography of a region. With this in mind, it would make sense to assume that the points closest to an unknown point would have the greatest influence on the unknown's head value. Thus, to simplify the data, only the unknown point and its five nearest known neighbors will be considered for these techniques.

A Simple Linear Method

The first technique used to calculate the unknown head values uses the two nearest co-linear points. To simplify calculations, only co-linear points along a constant X or constant Y gridline were considered. As a result, only two parameters will change—either the X or Y value, called l , and the head value, referred to as h . The point-slope equation of a line has been modified to reflect this notational change. Consider the slope of the line to be

$$m = \frac{\Delta h}{\Delta l} = \frac{h_1 - h_2}{l_1 - l_2} \quad (3.1)$$

The slope will be substituted into the point-slope equation of a line to yield the following equation

$$h - h_1 = m(l - l_1) \quad (3.2)$$

where (l_1, h_1) is any known point on the line. Once the equation of the line has been determined, it is possible to solve Equation 3.2 for any hydraulic head value h given its location l .

Consider Well A, located at (3000, 4000). The two nearest co-linear points are the wells located at (4000, 4000) and (3500, 4000) with hydraulic head values of 243.8-ft. and 250.0-ft., respectively. The slope of this line is

$$m = \frac{243.8 - 250.0}{3500 - 4000} = \frac{-6.2}{-500} = .0124.$$

Substituting this into the point-slope equation of the line, yields the equation

$$h - 243.8 = .0124(x - 3500)$$

$$h = .0124x + 200.4$$

which can be used to find the hydraulic head at A. Replacing the value of x with Well A's x value gives a hydraulic head value of

$$h = .0124(3000) + 200.4 = 237.6.$$

Table 3.2-1—The linear interpolation technique described by equations 3.1 and 3.2 has been used to approximate the hydraulic head values at points A, B, and C depicted in Figure 3.1-1. Points 1 and 2 refer to the two known wells used to calculate the slope m .

Location	Point 1			Point 2			Δh	Δl	m	Hydraulic Head Approx.
	x	y	h	x	y	h				
A (3000,4000)	3500	4000	243.8	4000	4000	250.0	-6.2	-500	.0124	237.6
B (3500,2000)	4500	2000	231.6	2500	2000	217.6	14	2000	.0070	224.6
C (1000,500)	3000	500	218.8	2500	500	215.7	3.1	500	.0062	206.4

The results of using this linear interpolation technique to solve for the unknown head values at points A, B, and C in Figure 3.1-1 are shown in Table 3.2-1.

Ranked Inverse Weighted Distance Method

After considering again the notion that the water table follows the topography of the land, it was thought that perhaps an inverse weighted distance method would interpolate the unknown head value more accurately. With inverse weighted distance methods, wells located nearer to the unknown point have greater influence on the value of the unknown hydraulic head than wells located farther away. Two different methods were developed using this concept.

The distance between each of the known wells and the unknown point were calculated. The n wells were then ranked d_1, d_2, \dots, d_n in order of increasing distance from the unknown point. The formula

$$h = \sum_{i=1}^n w_i h_i \quad (3.3)$$

where

$$w_i = \frac{d_{n-(i-1)}}{D} \quad (3.4)$$

and

$$D = \sum_{i=1}^n d_i, \quad (3.5)$$

was used to calculate h , the head value of the unknown well. Note that the sum of the weighting terms evaluates to 1.

Consider Well A once more. The wells closest to Well A are denoted in Table 3.2-2. Using only the first two wells, the distances can be ranked

$$d_1 = 500.00$$

$$d_2 = 707.11$$

$$D = 500 + 707.11 = 1207.11$$

thereby resulting in the weights

Table 3.2-2—The five wells closest to Well A, located at (3000, 4000), can be used to interpolate the hydraulic head value at A using the ranked inverse weighted distance method.

Well Location		Distance from Well A (3000, 4000)	Hydraulic Head Value
X	Y		
3500	4000	500.00	243.8
3500	4500	707.11	253.0
4000	4000	1000.00	250.0
2000	4500	1118.03	230.3
2500	3000	1118.03	222.2

$$w_1 = \frac{d_2}{D} = \frac{707.11}{1207.11}$$

$$w_2 = \frac{d_1}{D} = \frac{500.00}{1207.11}$$

The hydraulic head at A can then be calculated to be

$$h = w_1 h_1 + w_2 h_2$$

$$= \frac{707.11}{1207.11} (243.8) + \frac{500.00}{1207.11} (253.0)$$

$$= 247.6.$$

Inverse Weighted Distance Method

The second inverse weighted distance method that was developed uses a different weighting function. In this case, the distances between the known and unknown points are determined, but the wells do not necessarily need to be ranked in any particular order. To calculate the unknown h , the following formula was used:

$$h = \frac{\sum_{i=1}^n w_i h_i}{n-1} \quad (3.6)$$

where

$$w_i = 1 - \frac{d_i}{D} \quad (3.7)$$

and

$$D = \sum_{i=1}^n d_i . \quad (3.8)$$

Taking Well A into consideration once more, it can be seen that when using only two wells,

$$d_1 = 500.00$$

$$d_2 = 707.11$$

$$D = 500.00 + 707.11 = 1207.11$$

and

Table 3.2-3—Hydraulic head values have been calculated for points A, B, & C in Figure 3.1-1 using the 2 inverse weighted distance methods and varying numbers of wells.

Location	Number of Wells Used	Hydraulic Head Approximation	
		Inverse Weighted Distance Method 1 (Eq. 3.3-3.5)	Inverse Weighted Distance Method 2 (Eq. 3.6-3.8)
A	2	247.6	247.6
	3	248.2	248.6
	4	245.9	244.7
	5	242.9	240.4
B	2	222.7	222.7
	3	222.0	222.3
	4	223.9	224.5
	5	223.7	223.5
C	2	206.5	206.5
	3	207.8	207.4
	4	208.9	209.5
	5	210.1	211.2

$$w_1 = 1 - \frac{d_1}{D} = 1 - \frac{500.00}{1207.11} = .59$$

$$w_2 = 1 - \frac{d_2}{D} = 1 - \frac{707.11}{1207.11} = .41.$$

The hydraulic head value of A can then be calculated to be

$$\begin{aligned} h &= \frac{w_1 h_1 + w_2 h_2}{2 - 1} \\ &= \frac{.59(243.8) + .41(253.0)}{1} \\ &= 247.6. \end{aligned}$$

Table 3.2-3 summarizes the results of using the above two inverse weighted distance methods to determine the unknown head values. In order to illustrate how the number of wells affects the result, each method has been calculated using 2, 3, 4, and 5 wells.

Weighted Average of Nearby Points

These two inverse weighted distance methods are similar to a technique suggested by Hadlock. He proposes using a weighted average of nearby points. Pick the three points nearest the unknown point. If there is a fourth point at the same distance as one of the other three points, use that point as well. The unknown head value is calculated as the weighted average of these points' head values. The weighting factor is determined to be the reciprocal of the distances. Hadlock's method (1998b, p. 104) is as follows:

Chose n given points (x_i, y_i) . Then letting

$$r_i = \frac{1}{d_i} = \frac{1}{\text{distance between } (x,y) \text{ and } (x_i, y_i)} \quad (3.9)$$

each weighting factor would be given by

$$w_i = \frac{r_i}{\sum_{i=1}^n r_i} \quad (3.10)$$

so that the weighted average would be

$$z = \sum_{i=1}^n w_i z_i. \quad (3.11)$$

Consider Well A for one final time. The three closest wells will be used (refer to Table 3.2-2). Using these wells, the values of r would be

$$r_1 = \frac{1}{500.00} = .0020$$

$$r_2 = \frac{1}{707.11} = .0014$$

$$r_3 = \frac{1}{1000.00} = .0010$$

$$\sum_{i=1}^3 r_i = .0044$$

which would lead to the weights

$$w_1 = \frac{.0020}{.0044} = .4545$$

$$w_2 = \frac{.0014}{.0044} = .3182$$

$$w_3 = \frac{.0010}{.0044} = .2273.$$

The weighted average of these values, z , would then be

Table 3.2-4—Hadlock’s method of using a weighted average of nearby points has been used to determine the hydraulic head values at points A, B, and C in Figure 3.1-1.

<i>Well</i>	<i>Number of Wells Used</i>	<i>Head Approximation</i>
<i>A</i>	3	248.1
<i>B</i>	4	224.6
<i>C</i>	4	208.4

$$\begin{aligned}
 z &= w_1z_1 + w_2z_2 + w_3z_3 \\
 &= (.4545)(243.8) + (.3182)(253.0) + (.2273)(250.0) \\
 &= 248.1.
 \end{aligned}$$

Table 3.2-4 displays the results of calculating the unknown head values in this manner.

Advantages & Disadvantages

Although all four methods generated a value for the unknown hydraulic head, there were advantages and disadvantages to each method. The method of linear interpolation made use of nearby points, which are likely to be consistent with the unknown head value. While it is true that the water table should be continuous, the relationship may not be linear. In addition, the unknown point may not be co-linear with two known points. The two inverse weighted distance methods also had the advantage of taking into consideration nearby points. Unfortunately, the approximated head value will always stay within the range of the known points’ head values. This is not realistic if the unknown point happens to fall outside of the known points. Hadlock’s weighted average of nearby points has identical advantages and disadvantages. In addition, none of the methods discussed will provide a very smooth or continuous surface. As a result of these drawbacks, none of these methods were deemed robust enough to warrant further development.

3.3 Relaxation — Solving Finite-Difference Equations

One numerical method that has been developed to approximate the hydraulic head value at any point is relaxation, also known as the Gauss-Siedel method, the Liebmann method, or the method of successive displacements. This method requires the aquifer to be isotropic, have uniform composition, and constant hydraulic conductivity (K). This situation is three-dimensional, but flow in the z direction is negligible (Freeze & Cherry, 1979, chap. 5.3). Under these conditions, the hydraulic head function $h(x,y)$ must satisfy the two-dimensional Laplace equation, namely

$$h_{xx} + h_{yy} = 0. \tag{3.12}$$

The physical principle this equation describes is a basic conservation of mass condition: *the net fluid flow through an incremental volume of the aquifer at any moment must be 0* (Hadlock, 1998a, chap. 5.7).

Keep equation 3.12 in mind and recall a few concepts from elementary numerical analysis. Recall that the derivative of a function may be approximated as

$$f'(x) \approx \frac{f(x + \Delta x) - f(x - \Delta x)}{2\Delta x}. \tag{3.13}$$

Equation 3.13 is known as the central difference approximation to the derivative. A similar equation exists to approximate the second derivative, namely

$$f''(x) \approx \frac{f(x + \Delta x) - 2f(x) + f(x - \Delta x)}{(\Delta x)^2}. \tag{3.14}$$

This is called the central difference approximation to the second derivative (Hadlock, 1998a, chap.5.8).

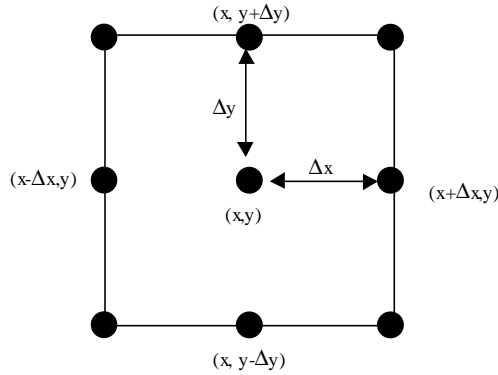


Figure 3.3-1—Grid points used to construct a numerical approximation to the partial derivatives at point (x, y) .

Suppose that a region under investigation has been sectioned into a grid and consider the situation portrayed by Figure 3.3-1. Suppose you want to determine the partial derivatives of the hydraulic head function $h(x, y)$ at the point (x, y) . Also assume you know the values of h at the additional points shown. Applying the central difference approximation to the second derivative, you see that

$$h_{xx}(x, y) \approx \frac{h(x + \Delta x, y) - 2h(x, y) + h(x - \Delta x, y)}{(\Delta x)^2} \quad (3.15)$$

$$h_{yy}(x, y) \approx \frac{h(x, y + \Delta y) - 2h(x, y) + h(x, y - \Delta y)}{(\Delta y)^2} \quad (3.16)$$

Equations 3.15 and 3.16 can then be substituted into Laplace's equation (equation 3.12) to yield

$$\frac{h(x + \Delta x, y) - 2h(x, y) + h(x - \Delta x, y)}{(\Delta x)^2} + \frac{h(x, y + \Delta y) - 2h(x, y) + h(x, y - \Delta y)}{(\Delta y)^2} = 0 \quad (3.17)$$

If an arbitrary grid is selected so that $\Delta x = \Delta y$ (i.e. the grid is square), then after simplification, equation 3.17 becomes

$$h(x, y) = \frac{h(x + \Delta x, y) + h(x, y - \Delta y) + h(x - \Delta x, y) + h(x, y + \Delta y)}{4} \quad (3.18)$$

Surprisingly enough, this tells us that the value of any unknown hydraulic head is simply the average of the four neighboring values (Hadlock, 1998a, chap. 5.8). Equation 3.18 is known as a finite-difference equation. Assuming that the boundaries of the grid are impermeable, equation 3.18 can be modified to determine the hydraulic head along the boundary line (eq. 3.19) or at a corner (eq. 3.20).

$$h(x, y) = \frac{h(x + \Delta x, y) + h(x - \Delta x, y) + 2h(x, y + \Delta y)}{4} \quad (3.19)$$

$$h(x, y) = \frac{2h(x - \Delta x, y) + 2h(x, y + \Delta y)}{4} \quad (3.20)$$

Figure 3.3-2 is a schematic representation of this finite-difference method (Freeze & Cherry, 1979, chap. 5.3).

If there are n nodes in the grid, then it is possible to develop n finite-difference equations in n unknowns. If n

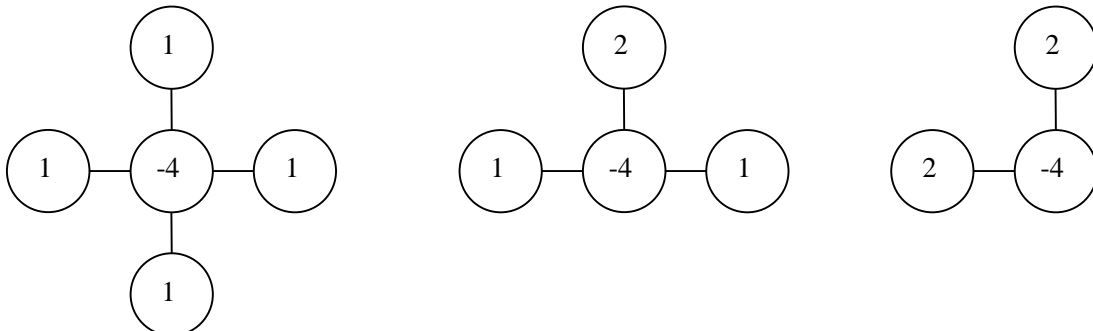


Figure 3.3-2—These finite difference stars are a schematic representation of the finite-difference method (Freeze & Cherry, 1979, fig. 5.12).

happens to be small, the equations could be solved directly, but in the case of a large grid it is more efficient to use relaxation. After assuming a starting value at each of the unknown points in the grid, one can sweep through the grid, left to right and top to bottom, applying the relevant finite-difference equation at each unknown point while keeping the known points fixed. The most recent calculation of the h value is always used. After every iteration, or pass, through the grid, the h values will begin to converge toward their final answers. A residual, r , may be calculated after an iteration to determine the difference in h between two successive iterations. That is,

$$r = |h_i - h_{i-1}|. \quad (3.21)$$

When the maximum residual has fallen below the predetermined tolerance level, that is when

$$r_{\max} < T, \quad (3.22)$$

the solution has been reached (Freeze & Cherry, 1979, chap. 5.3). It should be noted that this method is very robust. Regardless of how impractical the initial value of h seems, the values will always converge (Freeze & Cherry, 1979, chap. 5.3).

3.4 Test of Starting Conditions

Because the relaxation method can be used at any point in a grid, it is ideal for the situation posed by Hadlock. Using the data from Figure 3.1-1, Microsoft Excel spreadsheets were generated to calculate the hydraulic heads at all of the unknown points. Because no data was collected along the boundaries of the region, the boundaries were assumed instead to be along the 500 and 4500 gridlines. The tolerance level was set at 0.1 (i.e. the maximum residual had to be less than 0.1). Table 3.4-1 summarizes the number of iterations necessary to reach the tolerance when various starting values were assumed for the unknown points. The values 0, 225, and 250 were arbitrarily selected. The value 235.7 was assumed as an initial value because it is the mean of the minimum and maximum known head values.

It was noted that regardless of the initial h value, the finite-difference method eventually converged so that the residual was below the tolerance value. This observation prompted the following questions:

- What happens if we disregard known points in the interior of the grid and use only boundary data?
- What will happen if the unknown boundary points are interpolated using linear or cubic splines?
- If the boundary values have been interpolated, what occurs if the boundaries are or are not allowed to change?

In order to answer these questions, the relaxation method was tested on the ten cases that arose from the above questions. Table 3.4-2 summarizes the initial boundary and interior conditions that were altered in the tests. Spreadsheets were again created in Excel to calculate the unknown head values. The estimate used for the initial h values was the mean of the highest (268.2) and lowest (203.2) known values on the grid. Maple was used to interpolate the boundaries of the grid using linear and cubic splines.

Once all of the head values had been calculated, they were input into Maple to create two-dimensional hydraulic head contour maps. Due to the constraints of Maple, the data had to be read into the program from a text file. It was then manipulated to create lists of points—one list for each line in the grid in Figure 3.1-1. As a result, the scale on the contour maps is a reference to the grid line and does not directly reflect the geographic coordinate. For example, the origin (500, 500) falls at point (0, 0) while point (1500, 1500) is located at (2, 2).

Because Hadlock did not provide the actual hydraulic head contour map for the data in Figure 3.1-1 in his solution manual, a likely solution was provided by John Prendergast of the Bureau of Environmental Evaluation for the New Jersey Department of Environmental Protection. Prendergast generated a hydraulic head contour map from the initial data with Surfer for Windows. This program, created by The Scientific Software Group, is a three-dimensional contouring and surface plotting program used by engineers. The hydraulic head contour map seen in Figure 3.4-1 was created using the kriging method (Alley, 1993, pages 87-108), an interpolation method rooted in

Table 3.4-1—The relaxation method was used to calculate the unknown head values in Figure 3.1-1. The boundaries are assumed to be $500 \leq x \leq 4500$ and $500 \leq y \leq 4500$ (delineated by the dotted line in Figure 3.1-1). Various values were used as the initial guess for the unknown head values.

<i>Initial Value of Unknown Hydraulic Heads</i>	<i>Number of Iterations Needed</i>
0	20
225.0	11
235.7	13
250.0	14

Table 3.4-2—The relaxation method was initialized with varying amounts of data to simulate different boundary and interior point conditions. These variations cause a wide fluctuation in the number of iterations required to reach the predetermined tolerance level.

<i>Initialization Method</i>	<i>Unknown Boundary Estimate Used</i>	<i>Unknown Interior Point Estimate Used</i>	<i>Interior Known Point Used</i>	<i>Boundary Conditions</i>	<i>No. of Iterations Required</i>
1	235.7	235.7	235.7	Changing	32
2	235.7	235.7	Known	Changing	13
3	Linear spline	235.7	235.7	Changing	31
4	Linear spline	235.7	235.7	Fixed	22
5	Linear spline	235.7	Known	Changing	11
6	Linear spline	235.7	Known	Fixed	10
7	Cubic spline	235.7	235.7	Changing	31
8	Cubic spline	235.7	235.7	Fixed	22
9	Cubic spline	235.7	Known	Changing	11
10	Cubic spline	235.7	Known	Fixed	10

statistical analysis rather than numerical analysis (Surfer description, no date). This method is widely used by engineers and so was deemed an appropriate solution to the problem. Each of the ten contour maps generated in Maple (Figure 3.4-2 to Figure 3.4-11) was then visually compared with the contour map created in Surfer.

The visual comparison of the various contour maps generated interesting results. When all of the scattered data was used (method 2) and also when only scattered boundary data was used (method 1), the contour maps reflected the interior points accurately but displayed irregular results along the left boundary. The same problem occurred when unknown boundary points were approximated with linear or cubic splines and allowed to fluctuate (methods 3, 5, 7, and 9). When an estimate was used for all of the interior points and boundary values remained fixed at their linear or cubic approximations (methods 4 and 8), the contour maps were remarkably similar to the Surfer contour map. The most accurate contours were generated when all of the known interior points were used and a fixed boundary was created from linear or cubic splines (methods 6 and 10). These two methods also required the fewest number of iterations. Thus, methods 6 and 10 were deemed the best methods to interpolate this data set.

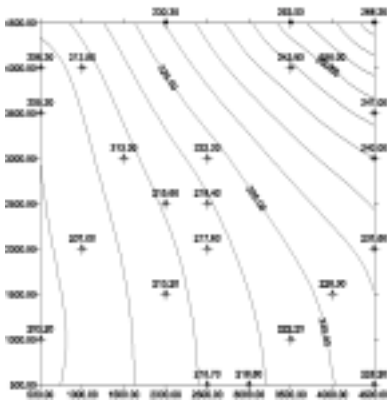


Figure 3.4-1—Contour map generated by Surfer for Windows using the kriging method.

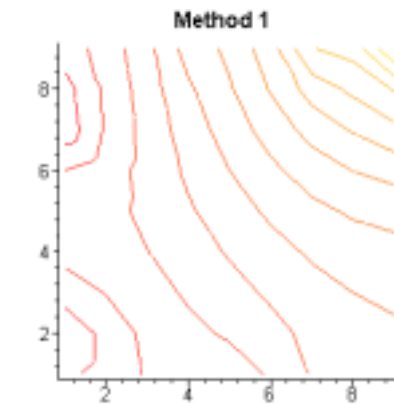


Figure 3.4-2—Estimates were used for unknown head values on the boundary and for all interior points. Boundary values were allowed to change. The values along the X and Y axes represent the grid lines (i.e. 2 would be 1500, 4 would be 2500, etc.).

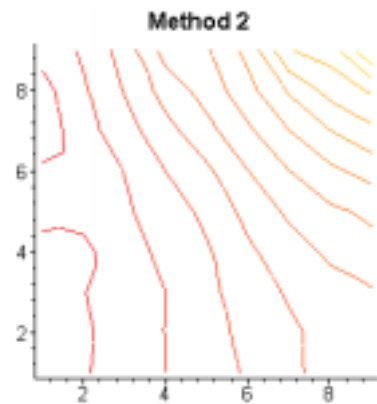


Figure 3.4-3—Estimates were used for the unknown head values on the boundary and the interior. Boundary values were allowed to change. The values along the X and Y axes represent the grid lines (i.e. 2 would be 1500, 4 would be 2500, etc.).

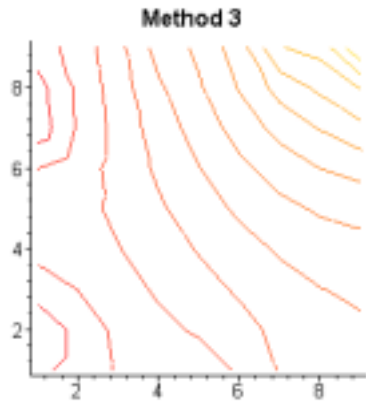


Figure 3.4-4—Estimates were used for all interior points and linear spline approximations were used for the boundary. Boundary values were allowed to change. The values along the X and Y axes represent the grid lines (i.e. 2 would be 1500, 4 would be 2500, etc.)

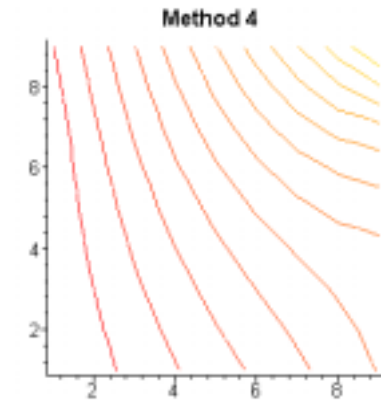


Figure 3.4-5—Estimates were used for all interior points and linear spline approximations were used for the boundary. Boundary values were not allowed to change. The values along the X and Y axes represent the grid lines (i.e. 2 would be 1500, 4 would be 2500, etc.).

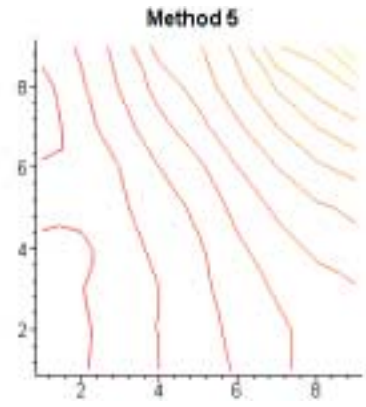


Figure 3.4-6—Estimates were used for unknown interior points and linear spline approximations were used for the boundary. Boundary values were allowed to change. The values along the X and Y axes represent the grid lines (i.e. 2 would be 1500, 4 would be 2500, etc.).

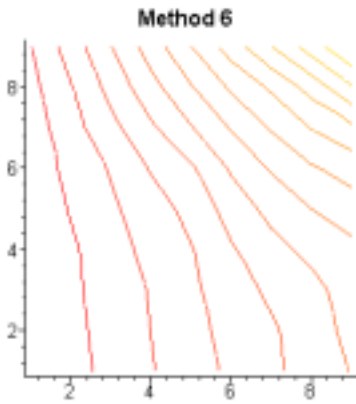


Figure 3.4-7—Estimates were used for unknown interior points and linear spline approximations were used for the boundary. Boundary values do not change. The values along the X and Y axes represent the grid lines (i.e. 2 would be 1500, 4 would be 2500, etc.).

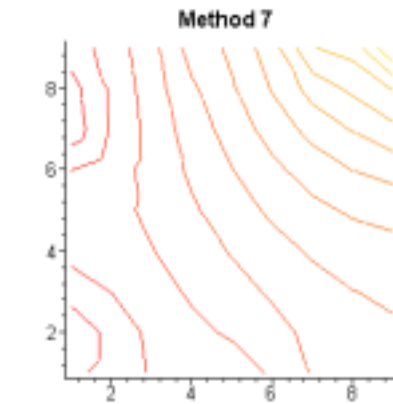


Figure 3.4-8—Estimates were used for all interior points and cubic spline approximations were used for the boundary. Boundary values were allowed to change. The values along the X and Y axes represent the grid lines (i.e. 2 would be 1500, 4 would be 2500, etc.).

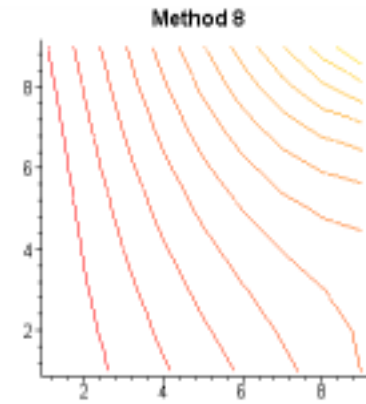


Figure 3.4-9—Estimates were used for all interior points and cubic spline approximations were used for the boundary. Boundary values were not allowed to change. The values along the X and Y axes represent the grid lines (i.e. 2 would be 1500, 4 would be 2500, etc.).

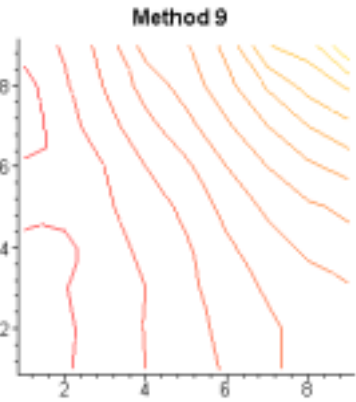


Figure 3.4-10—Estimates were used for unknown interior points and cubic spline approximations were used for the boundary. Boundary values do not change. The values along the X and Y axes represent the grid lines (i.e. 2 would be 1500, 4 would be 2500, etc.).

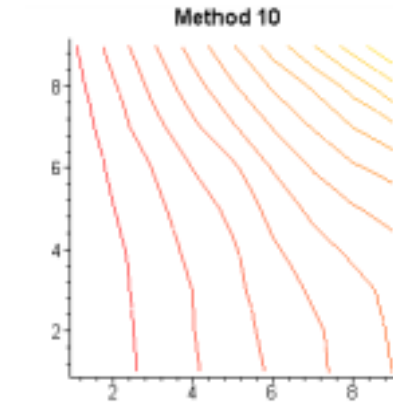


Figure 3.4-11—Estimates were used for unknown interior points and cubic spline approximations were used for the boundary. Boundary values do not change. The values along the X and Y axes represent the grid lines (i.e. 2 would be 1500, 4 would be 2500, etc.).

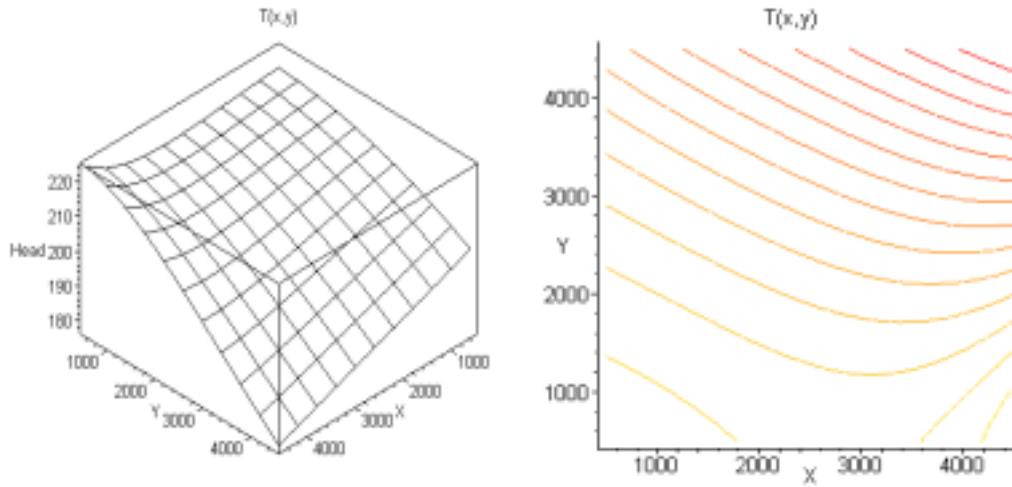


Figure 3.5-1—Three-dimensional view (left) and contour map (right) of the exponential test function $T(x,y)$.

3.5 Relaxation Method Applied to Known Test Functions

Although it was possible to calculate the unknown head values and create a hydraulic head contour map for Hadlock's problem, the actual head values at each point are not known. The visual comparison of the ten generated contour maps with the Surfer map did not seem sufficient enough to gauge the accuracy of varying the initial conditions in the finite-difference method. Thus, two known functions were selected to create a situation similar to that presented by Hadlock. The functions were chosen because of their resemblance to head contour diagrams seen in various modeling texts. Each function was graphed in two and three dimensions and various points were chosen to serve as the known data.

The first function chosen to serve as a test function was

$$T(x, y) = 20e^{\left(\frac{x}{5000}\right)^3} - 2\left(\frac{x}{5000}\right)\left(\frac{y}{5000}\right)^2 - \left(\frac{x}{5000}\right)^2 - \left(\frac{y}{5000}\right)^2 + 200. \quad (3.23)$$

It was evaluated on the range $0 \leq x \leq 5000$ and $0 \leq y \leq 5000$ and graphed on an 11 x 11 grid (see Figure 3.5-1). Twenty-four points, seen in Figure 3.5-2, were selected to serve as the known data points. These known head values range from a low of 177.2 to a high of 224.3 within the range $500 \leq x \leq 4500$ and $500 \leq y \leq 4500$.

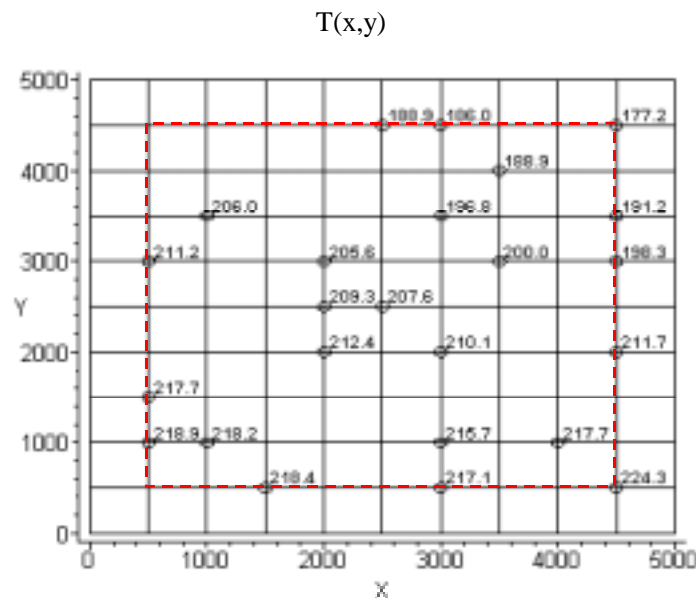


Figure 3.5-2—Each of the 24 points marked indicates a known head value. The dotted line marks the boundaries used. All other points within the boundary are considered unknown.

Table 3.5-1— Summary of results using the various finite-difference methods to approximate unknown points on the exponential function $T(x,y)$.

Method #	Initial Conditions Used	No. of Iterations	Mean Absolute Error	Mean Relative Error
1	200.75 used for unknown head values on boundary and for all interior points. Boundary values allowed to change.	23	1.712	.008
2	200.75 used for unknown head values on boundary and in interior. Boundary values allowed to change.	12	.940	.005
3	200.75 used for all interior points. Linear spline approximations used for boundary. Boundary values allowed to change.	22	1.812	.009
4	200.75 used for all interior points. Linear spline approximations used for boundary. Boundary values not allowed to change.	20	.812	.004
5	200.75 used for unknown interior points. Linear spline approximations used for boundary. Boundary values allowed to change.	12	.935	.005
6	200.75 used for unknown interior points. Linear spline approximations used for boundary. Boundary values not allowed to change.	9	.297	.001
7	200.75 used for all interior points. Cubic spline approximations used for boundary. Boundary values allowed to change.	22	1.813	.009
8	200.75 for all interior head values. Cubic spline approximations used for boundary. Boundary values not allowed to change.	20	.752	.004
9	200.75 for unknown interior points. Cubic spline approximations used for boundary. Boundary values allowed to change.	12	.935	.005
10	200.75 for unknown interior head values. Cubic spline approximations used for boundary. Boundary values not allowed to change.	9	.249	.001

The finite-difference methods discussed above were then used to calculate all of the unknown head values on the grid. The mean of the minimum and maximum head values, 200.75, was used as the initial estimate of h . Once again, Maple was used to generate linear and cubic spline approximations to the boundaries. The tolerance was set to 0.1.

Once values had been determined for all of the unknown points, contour maps were generated so that a visual analysis could be made of the accuracy of the data generated. In addition to conducting a visual comparison of the contour maps, it was possible to actually calculate the absolute and relative errors at each point approximated. Table 3.5-1 compares the effect of the various initial conditions on the average absolute and relative errors, as well as the number of iterations required to reach the tolerance.

The function chosen to serve as the second test function,

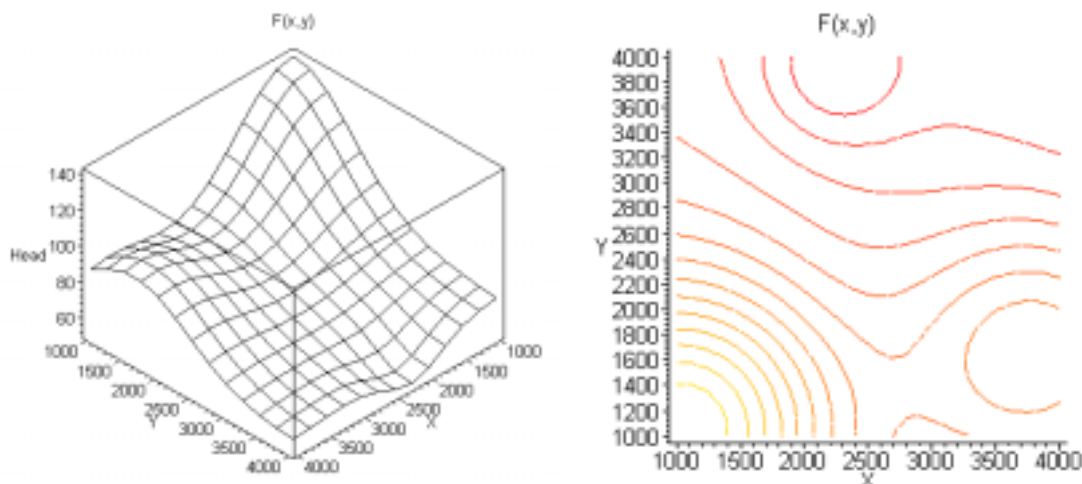


Figure 3.5-3—Three-dimensional view (left) and contour map (right) of $F(x,y)$, the modified Franke's function.

F(x,y)

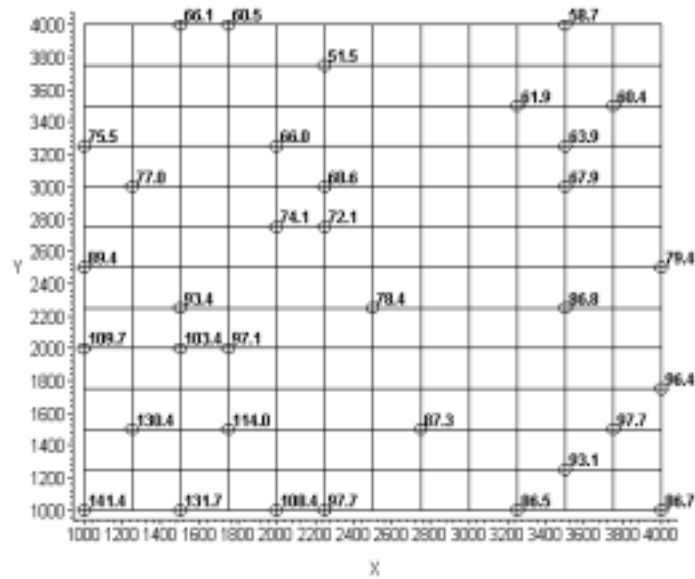


Figure 3.5-4—The 34 points marked are the known points that will be used for the modified Franke's function F(x,y).

$$F(x, y) = 75 \left(\frac{3}{4} e^{-\frac{1}{4} \left[\left(\frac{9x}{5000} - 2 \right)^2 + \left(\frac{9y}{5000} - 2 \right)^2 \right]} + \frac{3}{4} e^{-\left[\frac{1}{49} \left(\frac{9x}{5000} + 1 \right)^2 + \frac{1}{10} \left(\frac{9y}{5000} + 1 \right)^2 \right]} - \frac{1}{5} e^{-\left[\left(\frac{9x}{5000} - 4 \right)^2 + \left(\frac{9y}{5000} - 7 \right)^2 \right]} + \frac{1}{2} e^{-\frac{1}{4} \left[\left(\frac{9x}{5000} - 7 \right)^2 + \left(\frac{9y}{5000} - 3 \right)^2 \right]} \right) + 50 \quad (3.24)$$

is a modification of a function used by Richard Franke to test various scattered data interpolation methods (Hoschek & Lasser, 1989/1993, p. 419). Although Franke's function is ordinarily evaluated on a unit square, for our purposes it

Table 3.5-2— Summary of results using the various finite-difference methods to approximate unknown points on the modified Franke's function F(x,y).

Method #	Initial Conditions Used	No. of Iterations	Mean Absolute Error	Mean Relative Error
1	96.45 used for unknown head values on boundary and for all interior points. Boundary values allowed to change.	53	7.961	.112
2	96.45 used for unknown head values on boundary and in interior. Boundary values allowed to change.	23	1.735	.022
3	96.45 used for all interior points. Linear spline approximations used for boundary. Boundary values allowed to change.	49	7.985	.112
4	96.45 used for all interior points. Linear spline approximations used for boundary. Boundary values not allowed to change.	38	4.941	.066
5	96.45 used for unknown interior points. Linear spline approximations used for boundary. Boundary values allowed to change.	23	1.733	.022
6	96.45 used for unknown interior points. Linear spline approximations used for boundary. Boundary values not allowed to change.	19	2.034	.026
7	96.45 used for all interior points. Cubic spline approximations used for boundary. Boundary values allowed to change.	49	7.977	.112
8	96.45 for all interior head values. Cubic spline approximations used for boundary. Boundary values not allowed to change.	40	3.825	.051
9	96.45 for unknown interior points. Cubic spline approximations used for boundary. Boundary values allowed to change.	23	1.733	.022
10	96.45 for unknown interior head values. Cubic spline approximations used for boundary. Boundary values not allowed to change.	19	1.576	.021

has been modified and evaluated on the range $1000 \leq x \leq 4000$ and $1000 \leq y \leq 4000$ (see Figure 3.5-3). Because a larger grid work was chosen (13 x 13), 34 known points were selected rather than 24 (see Figure 3.5-4). Head values ranged from 51.5 to 141.4, which meant the estimate used for the initial h was 96.45. A tolerance of 0.1 is used. summarizes the effect the initial conditions have on average errors and the number of iterations required to reach the tolerance.

A visual analysis revealed that initialization methods 6 and 10 produced the most accurate contour lines for the exponential test function $T(x,y)$. Reviewing the average absolute and relative errors confirmed this since these methods produced the two lowest errors. In addition, methods 6 and 10 yielded solutions after the fewest iterations. Thus, the most accurate contours for $T(x,y)$ were generated when the initial data set had a stationary boundary and scattered interior points.

Because the contours produced by the modified Franke's test function $F(x,y)$ were so complex, the results were not as accurate. Some of the contours reflected wild fluctuations in height. When none of the interior data was used the contours created were smooth, but not at all accurate. It was ultimately decided that initialization methods 10, 9, and 5 (in that order) generated the most visually accurate contours. These results were confirmed by comparing the average relative and absolute errors and the number of iterations required. Thus the best results were achieved when the initial data either had a stationary boundary created from a cubic spline or had a changing boundary created from linear or cubic spline approximations. All three cases used the known interior data points.

3.6 Relaxation Method Applied to Real Data

Once testing had been done on the two known functions, it seemed reasonable to attempt to test the relaxation on a collection of real data obtained from the Bureau of Environmental Evaluation for the New Jersey Department of Environmental Protection. This data, presented in a Microsoft Excel spreadsheet, summarized the information collected from 83 wells at an undisclosed location in New Jersey. The file contains the state plane coordinates for each of the wells in feet, as well as the height of the well casing and the May 1998 groundwater elevation in feet. This groundwater elevation refers not the hydraulic head, but instead to simply the depth of the water in the well. In order to find the actual hydraulic head values, it was necessary to add the May 1998 groundwater elevations to the height of the well casing. This yielded known hydraulic head elevations ranging from a low of 9.6-ft to a high of 80.4-ft above sea level.

The locations of the 83 wells were then plotted to determine if all of the data should be used or simply a portion of it. When the data was plotted, it was clustered in two distinct regions. After decreasing the grid size from a 500-ft by 500-ft grid down to a 50-ft by 50-ft grid, it appeared that the 37 wells in the eastern region of the graph lie closer to actual grid points. This was important to consider since the relaxation method requires that the hydraulic head values lie on the grid points of a square grid. Because the eastern subset of wells appeared to be closer to grid points than the western subset, it was thought that this subset might be easier to work with for some initial tests. The subset of wells ultimately selected for testing have hydraulic head values between 30.7-ft and 71.4-ft within the range $1911669.7 \leq x \leq 1913541.8$ and $427579.5 \leq y \leq 432001.7$.

Using a 50-ft by 50-ft grid, the 37 eastern wells were clustered around 24 distinct grid points. Because none of the known values was located on grid points, it was necessary to interpolate the hydraulic head values for these 24 grid points. I decided to interpolate the values of the hydraulic heads at only these points using Hadlock's weighted average of nearby points. Following the methodology set forth in Section 3.2, the three wells closest to each grid point were used to calculate weighting factors that could be used to calculate a hydraulic head value for the grid point. These interpolated hydraulic head values will serve as the known values for the relaxation methods.

The plot that was generated by these interpolated points had only a single point on each of the boundaries. Because the linear spline method of interpolation requires at least two points, and the cubic spline method requires at least three points, it was necessary to further modify the initial data set. As a result, three of the outlying known values were discarded from the data set so that boundaries could be calculated easily using linear and cubic splines. This left three of the four boundaries with only a single point on the boundary, but the remaining edge, the line $x = 1913050$, had three known values located on it. The importance of starting with this side is discussed shortly. The remaining values are located in a region ranging from $1911650 \leq x \leq 1913050$ and $428950 \leq y \leq 431950$ (see Figure 3.6-1).

Rather than testing all ten of the initialization methods that had been developed, only methods 2, 5, 6, 9 and 10 were tested. Method 2 was chosen based on the fact that this was the exact situation portrayed by the real data—there were scattered points on the boundary and in the interior of the region. The remaining four methods were tested because they had been deemed the most accurate methods based on visual comparison and an error analysis.

In order to test methods 5, 6, 9 and 10, boundaries were calculated in Maple using linear and cubic splines. The splines were interpolated in a counter-clockwise manner (i.e. the eastern, northern, western, and southern

boundaries were calculated in that order). By splining the boundaries in this manner, it was possible to obtain a complete spline through the eastern boundary, which had three known points. From this spline, a second known value for the northern boundary could be determined using the northern-most endpoint of the eastern boundary. Subsequent splinings made it possible to determine a second known point on the other boundaries and then calculate the full boundary lines.

The original splined boundaries that were calculated generated points that diminished the precision of the calculations. It was determined that this was due to numerical error. As a result, it necessary to increase the precision used to calculate the splines. It was also hypothesized that perhaps the range of results might be narrowed by splining the boundaries in a clockwise manner (first eastern, then southern, western, and northern boundary lines). Thus, an alternate set of splined boundaries was also calculated to see what effect they would have on the test methods. These alternate boundaries are noted in the name of the test methods with the addition of the letter “a” to the test number.

After splines had been calculated, spreadsheets were generated in Microsoft Excel in order to test the five methods. As with earlier tests, the tolerance level was set to 0.1. The mean of the minimum and maximum values, 45.55-ft, was used as the initial estimate of h . Values were then calculated for each of the unknown grid points in the region.

Eastern Subset--Interpolated Initial Data

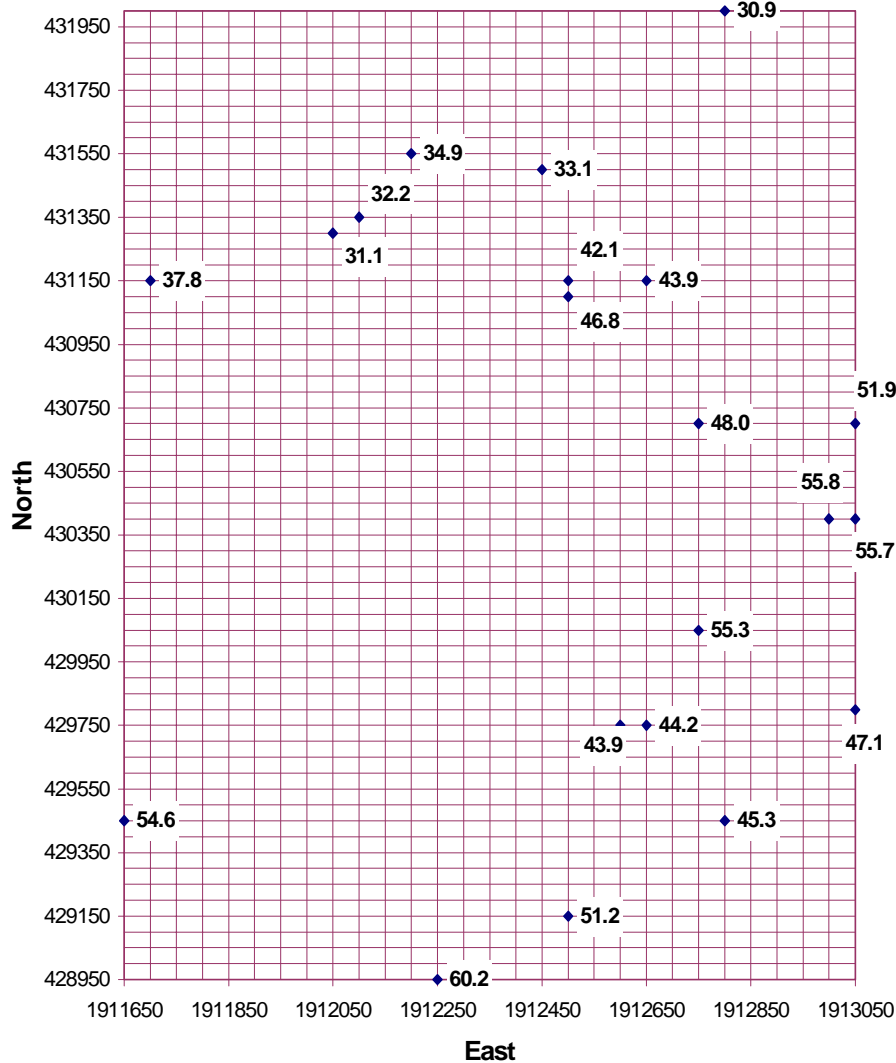


Figure 3.6-1 –Using the weighted average of nearby points discussed in Section 3.2, it was possible to interpolate hydraulic head values for the 21 grid points that the 37 wells in the eastern region were clustered around.

Maple was used to generate contour maps for each of the different scenarios (see Figure 3.6-2 to Figure 3.6-10) and a visual comparison of the various methods was made. Since there was no “accepted solution” provided with this data, I decided to use the contour map that resulted from testing Method 2 as the basis for comparison. This map is the result of using the known data without any boundary interpolation. All of the other contour maps were compared to this map with the focus on consistency, since accuracy cannot be judged.

The visual comparison of the nine contour maps yielded some interesting results. Overall, the linear methods (5, 5a, 6, and 6a) were pretty similar to their cubic counterparts (9, 9a, 10, and 10a). This was due to the fact that initial data on the boundaries was sparse so the cubic splines that were calculated for the boundaries decomposed into linear splines, although the decomposed cubic splines were not the same as the linear splines. The contours generated by Method 5 and 5a (recall that they use scattered interior data and a changing linear splined boundary) are quite similar to Method 2’s contours. As can be seen by comparing Method 5 with 5a, the change in the order in which the

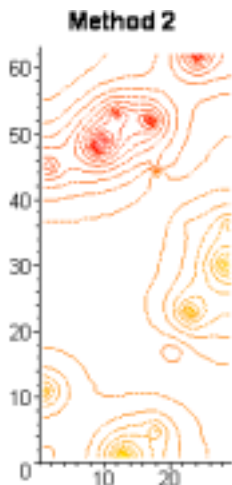


Figure 3.6-2 - Estimates were used for the unknown head values on the boundary and the interior. Boundary values were allowed to change. The values along the X and Y axes represent the number of the grid lines rather than the coordinate value.

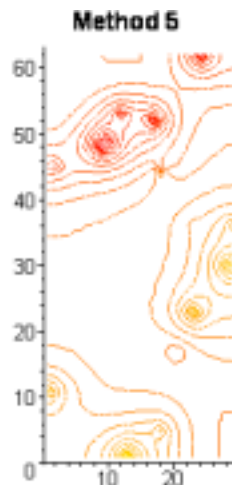


Figure 3.6-3 - Estimates were used for unknown interior points and linear spline approximations were used for the boundary. Boundary values were allowed to change. Boundaries were calculated in a counter-clockwise manner. The values along the X and Y axes represent the number of the grid lines rather than the coordinate value.

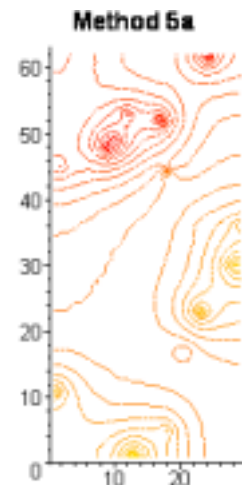


Figure 3.6-4 - Estimates were used for unknown interior points and linear spline approximations were used for the boundary. Boundary values were allowed to change. Boundaries were calculated in a clockwise manner. The values along the X and Y axes represent the number of the grid lines rather than the coordinate value.

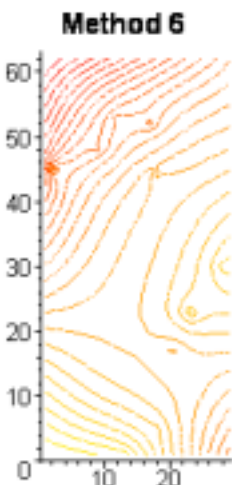


Figure 3.6-5 - Estimates were used for unknown interior points and linear spline approximations were used for the boundary. Boundary values were not allowed to change. Boundaries were calculated in a counter-clockwise manner. The values along the X and Y axes represent the number of the grid lines rather than the coordinate value.

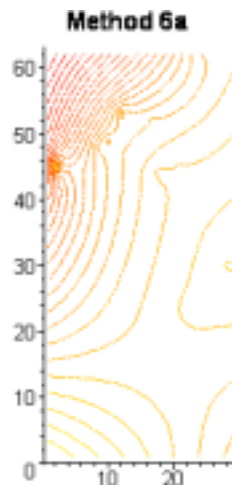


Figure 3.6-6 - Estimates were used for unknown interior points and linear spline approximations were used for the boundary. Boundary values were not allowed to change. Boundaries were calculated in a clockwise manner. The values along the X and Y axes represent the number of the grid lines rather than the coordinate value.

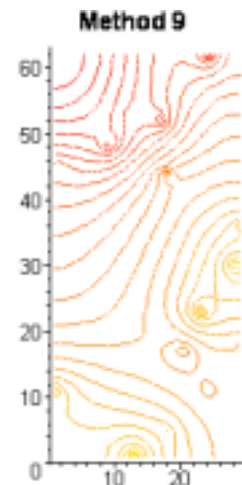


Figure 3.6-7 - Estimates were used for unknown interior points and cubic spline approximations were used for the boundary. Boundary values were allowed to change. Boundaries were calculated in a counter-clockwise manner. The values along the X and Y axes represent the number of the grid lines rather than the coordinate value.

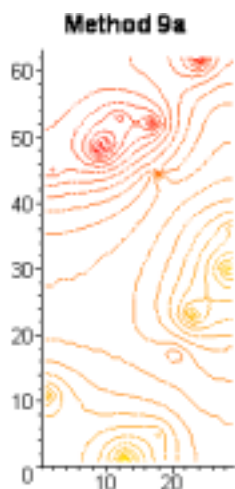


Figure 3.6-8 - Estimates were used for unknown interior points and cubic spline approximations were used for the boundary. Boundary values were allowed to change. Boundaries were calculated in a clockwise manner. The values along the X and Y axes represent the number of the grid lines rather than the coordinate value.

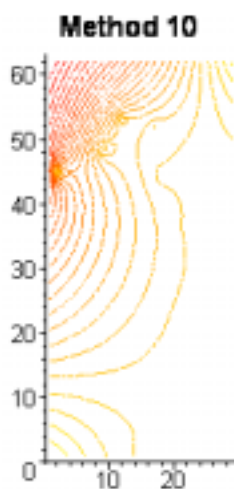


Figure 3.6-9 - Estimates were used for unknown interior points and cubic spline approximations were used for the boundary. Boundary values were not allowed to change. Boundaries were calculated in a counter-clockwise manner. The values along the X and Y axes represent the number of the grid lines rather than the coordinate value.

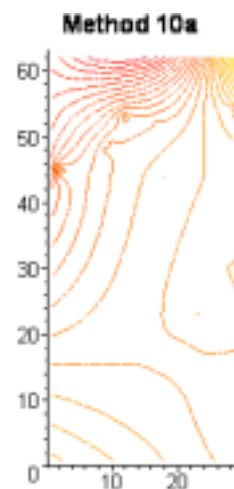


Figure 3.6-10 - Estimates were used for unknown interior points and cubic spline approximations were used for the boundary. Boundary values were not allowed to change. Boundaries were calculated in a clockwise manner. The values along the X and Y axes represent the number of the grid lines rather than the coordinate value.

boundaries were splined in has little effect on the contours. The contours from Methods 6 and 6a, as well as 10 and 10a, are very inconsistent with the contours from Method 2. Recall that all four of these methods used a fixed splined boundary. The contours generated from Methods 9 and 9a, unlike the other methods, were more dissimilar from each other than the alternate methods. The contours generated by Method 9 (recall that it used scattered interior data and a changing cubic splined boundary that had been calculated in a counter-clockwise manner) were less consistent with Method 2's contours than Method 9a (which had the same starting conditions as 9, except the boundaries were calculated in a clockwise manner). Thus it is interesting to see the effect that changing the direction of the splining has on the contours. The ultimate conclusion was that Methods 5, 5a, and 9 were most consistent with Method 2's contours.

4 Summary of Results

Based on a visual analysis of the hydraulic head contour maps generated for Hadlock's problem (see Figure 3.1-1 and Figure 3.4-2 through Figure 3.4-11), the data initialization methods 6 and 10 most accurately reflected the contours generated by Surfer. These methods were initialized with the known interior data and the boundary, generated from either linear or cubic spline approximations, did not change.

A similar visual analysis was conducted on the two test functions. Three additional factors—average absolute error, average relative error, and number of iterations needed—were taken into consideration to determine which was the ideal initial data set. Given these criteria, it was apparent that methods 6 and 10 again generated the best looking and most accurate set of hydraulic head contour lines for the exponential test function $T(x,y)$. Because the modified Franke's test function $F(x,y)$ generated a more complex surface, it was somewhat more difficult to select a best visual representation. After careful consideration, initialization methods 10, 9, and 5 (in that order) generated the best hydraulic head contour maps. Analysis of the average errors and number of iterations confirmed the visual results.

Given the results of generating hydraulic head contour lines for Hadlock's problem and the two test functions, it appears that initialization method 10 produces the best results. That is, the most accurate contour lines can be generated when the data set contains an stationary boundary, scattered interior points, and an estimate is used for the unknown interior points. If data is not available for all of the boundary points, a suitable replacement would be to generate a boundary from cubic splines between the known boundary points.

The above results were inconsistent with the results of testing the initialization methods on real data. Based on a visual comparison of the contours generated by Methods 2, 5, 6, 9, and 10, the best methods were Methods 2, 5, and 9, in particular 5 and 9 when the boundaries were splined in a clockwise manner. In prior tests, it appeared that the methods in which a cubic spline was used and then held constant yielded better, more accurate contours, than other methods. With the real data tested, this was not the case. Overall, it would appear that there are still large

inconsistencies in the results. Much more work needs to be done in order to draw definite conclusions about testing the methods with real data.

5 Future Study

The interpolation methods suggested in this paper are a convenient springboard for additional work. The inverse weighted distance methods presented in Section 3.2 are similar to Shepard's method, an inverse weighted distance method developed by geologists and meteorologists (Hoschek & Lasser, 1989/1993, chap. 9.1). It would be interesting to see what effect using Shepard's method would have on the hydraulic head contour lines. In addition, the relaxation method discussed in Section 3.3 can be modified by introducing an additional variable. This method, called successive overrelaxation, can reduce the number of iterations required to reach a solution, thereby making it more efficient than relaxation.

A number of software packages are available for generating contour maps from scattered data. Although the majority are intended for industrial use, making their use cost-prohibitive for this work, a few more economical software packages do exist. Continued work on this project might include a study of how the contour maps generated for this paper compare with those produced by contouring software, such as the Surface III software package created by the Kansas Geological Survey. This could be very beneficial in determining why there are such discrepancies between the real data tests and other tests.

Because of the inconsistency of the results of the real data tests, further work should be conducted on this data. Perhaps more known points or a larger grid, or both, are needed to improve consistency. It would be interesting to see how the successive overrelaxation method and Shepard's method affect the contours for real data. Lastly, and perhaps most importantly, further study will investigate how the hydraulic head contour maps that are generated affect groundwater flow paths.

References

- Alley, W. M. (1993). Geostatistical Models. In W. M. Alley (Ed.), *Regional Ground-Water Quality* (pages. 87 - 108)., Van Nostrand Reinhold.
- Freeze, R. A., & Cherry, J. A. (1979). Groundwater. Upper Saddle River, NJ: Prentice Hall.
- Hadlock, C. H. (1998a). Mathematical modeling in the environment. USA: The Mathematical Association of America.
- Hadlock, C. H. (1998b). Supplementary material and solutions manual for mathematical modeling in the environment. USA: The Mathematical Association of America.
- Hoschek, J., & Lasser, D. (1993). Computer aided geometric design. (L. L. Schumaker, Trans.). Wellesly, MA: A K Peters, Ltd. (Original work published 1989)
- Knapp, K. M. (1999). The interpolation of hydraulic head contours. Unpublished honors thesis, Ursinus College.
- Stewart, J. (1995). Calculus (3rd ed.). New York: Brooks/Cole Publishing Company.
- Surfer description [Online]. (No date). Available: http://www.scisoftware.com/products/surfer_details/surfer_details.html [1999. July 1].